The C–I···X$^-$ halogen bonding of tetraiodoethylene with halide anions in solution and cocrystals investigated by experiment and calculation

*Hui Wang, Xiao Ran Zhao and Wei Jun Jin**

College of Chemistry, Beijing Normal University, Beijing 100875, P. R. China.

Tel/Fax: (+86)10-58802146, E-mail: wjjin@bnu.edu.cn

Supporting Information

In solution

The deriving process of the formula:

If the complexes have 1:n binding stoichiometry, the equilibrium can be described as in equation:[1]

$$[D] + n[A] \rightleftharpoons DA_n$$

The equilibrium constant (K_a) is then expressed as

$$K_a = \frac{DA_n}{[D]\,[A]^n} \qquad (1)$$

According to the conservation of mass

$$[D] + [DA_n] = [D]_0 \qquad (2)$$

$$[A] + n[DA_n] = [A]_0 \qquad (3)$$

If $[A]_0 >> [D]_0$, the equation (3) can be replaced with $[A]=[A]_0$.

Rearrange the resulting equation, and the relation is obtained:

$$[DA_n] = \frac{K_a\,[D]_0\,[A]_0{}^n}{1 + K_a\,[A]_0{}^n} \qquad (4)$$

Where $[D]_0$, $[A]_0$ is the initial concentration of donor and acceptor, $[DA_n]$ is the equilibrium concentration of the formed XB complexes. In the process of UV-Vis titration acetonitrile as a typical solvent, the total absorbance (Abs) of the various absorption species in solution can be expressed as:

$$\begin{aligned}\mathrm{Abs} &= \varepsilon_{\mathrm{D}} b[\mathrm{D}] + \varepsilon_{\mathrm{DAn}} b[\mathrm{DA_n}] + \varepsilon_{\mathrm{A}} b[\mathrm{A}] \\ &= \varepsilon_{\mathrm{D}} b\,([\mathrm{D}]_0 - [\mathrm{DA_n}]) + \varepsilon_{\mathrm{DAn}} b[\mathrm{DA_n}] + \varepsilon_{\mathrm{A}} b\,([\mathrm{A}]_0 - \mathrm{n}[\mathrm{DA_n}]) \\ &= \varepsilon_{\mathrm{D}} b[\mathrm{D}]_0 - \varepsilon_{\mathrm{D}} b[\mathrm{DA_n}] + \varepsilon_{\mathrm{DAn}} b[\mathrm{DA_n}] + \varepsilon_{\mathrm{A}} b[\mathrm{A}]_0 - \mathrm{n}\varepsilon_{\mathrm{A}} b[\mathrm{DA_n}] \\ &= \varepsilon_{\mathrm{D}} b[\mathrm{D}]_0 + \varepsilon_{\mathrm{A}} b[\mathrm{A}]_0 + (\varepsilon_{\mathrm{DAn}} - \varepsilon_{\mathrm{D}} - \mathrm{n}\varepsilon_{\mathrm{A}}) b[\mathrm{DA_n}]\end{aligned}$$

If $\mathrm{Abs}_0 = \varepsilon_{\mathrm{D}} b[\mathrm{D}]_0 + \varepsilon_{\mathrm{A}} b[\mathrm{A}]_0$

$$\Delta\mathrm{Abs} = \mathrm{Abs} - \mathrm{Abs}_0 = (\varepsilon_{\mathrm{DAn}} - \varepsilon_{\mathrm{D}} - \mathrm{n}\varepsilon_{\mathrm{A}}) b[\mathrm{DA_n}] = \Delta\varepsilon b[\mathrm{DA_n}]$$

After the arrangement,

$$\frac{b[\mathrm{D}]_0}{\Delta\mathrm{Abs}} = \frac{1}{K_{\mathrm{a}}\varepsilon[\mathrm{A}]_0^{\mathrm{n}}} + \frac{1}{\varepsilon} \qquad (5)$$

So, K_{a} and ε can be obtained by the double-reciprocal curve (5).

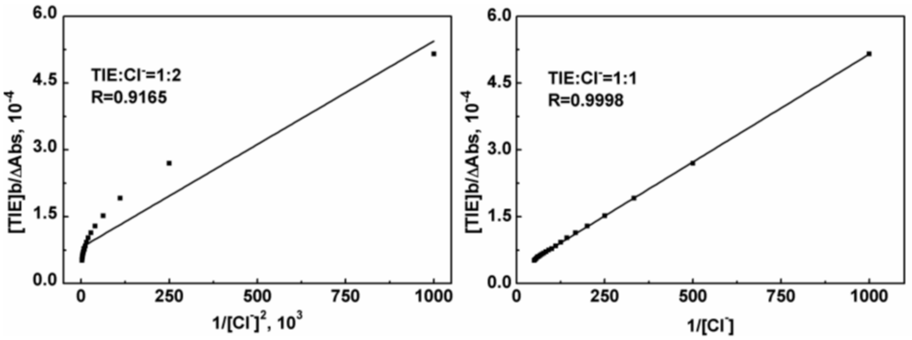

Fig. S1 Plots of [TIE]*b*/ΔAbs *vs.* 1/[Cl$^-$]^n in the differential spectrophotometric method.

In cocrystal

Table S1 Cocrystal data and structure refinement of TIE/X$^-$ complexes

compound reference	TIE	TIE/Cl$^-$	[a] TIE/Br$^-$	[b] TIE/Br$^-$	TIE/I$^-$
chemical formula	C_2I_4	$C_{22}H_{36}ClI_{12}N$	$C_{22}H_{36}BrI_{12}N$	$C_{18}H_{36}BrI_4N$	$C_{18}H_{36}I_5N$
formula Mass	531.62	1872.77	1917.23	853.99	900.98
crystal system	Monoclinic	Tetragonal	Tetragonal	Triclinic	Triclinic
a/Å	14.979(3)	15.9134(8)	16.0167(7)	13.4297(11)	9.003(3)
b/Å	4.3028(8)	15.9134(8)	16.0167(7)	14.0614(12)	9.062(3)
c/Å	12.748(2)	17.0463(18)	17.0905(15)	15.1348(13)	19.036(7)
α/°	90.00	90.00	90.00	98.1200(10)	81.642(6)
β/°	108.508(3)	90.00	90.00	101.3600(10)	80.716(6)
γ/°	90	90.00	90.00	106.2410(10)	64.652(6)
unit cell volume/Å^3	779.1(3)	4316.7(5)	4384.3(5)	2631.1(4)	1380.0(9)
temperature/K	110(2)	110(2)	120(2)	110(2)	110(2)
space group	P2(1)/c	I4/mmm	I4/mmm	P-1	P-1
No. of formula units per unit cell, Z	4	4	4	4	2
No. of reflections measured	3335	10965	10712	13160	6588
No. of independent reflections	1393	1148	1161	9423	4768
R_{int}	0.0315	0.0425	0.0401	0.0214	0.0613
final R_1 values ($I > 2\sigma(I)$)	0.0397	0.0517	0.0513	0.0337	0.0778
final $wR(F^2)$ values ($I > 2\sigma(I)$)	0.0886	0.1305	0.1363	0.0699	0.2239
final R_1 values (all data)	0.0413	0.0571	0.0557	0.0435	0.0911
final $wR(F^2)$ values (all data)	0.0893	0.1342	0.1406	0.0742	0.2441

[a] from acetonitrile, dichloromethane and the mixture of dichloromethane-ethanol (5:1), respectively. [b] from acetone, others from the four different solvents.

Table S2 Component and bonding stoichiometries of TIE/X$^-$ cocrystals

cocrystals	TIE/Cl$^-$			TIE/Br$^-$					TIE/I$^-$	
	from 4 solvents			from acetone		from other 3 solvents			from 4 solvents	
component			3:1		1:1			3:1		1:1
	C–I···Cl$^-$		2:1			C–I···Br$^-$		2:1		
bonding	C–I···π		1:1	C-I···Br$^-$	1:1	C–I···π		1:1	C–I···I$^-$	1:1
	C–I···I–C	type-I	1:1			C–I···I–C	type-I	1:1		
		type-II	1:2				type-II	1:2		

Table S3 Bonding properties and geometrical parameters of TIE/Br$^-$ cocrystal prepared from acetone

interactions	d/Å	θ/°
C–1I···1Br$^-$	3.354(1) (-14.7%)	170.3(1)
C–1I′···1Br$^-$	3.354(1)	158.7(0)
C–4I···1Br$^-$	3.321(1) (-15.5%)	174.2(1)
C–4I′···1Br$^-$	3.321(1)	159.1(0)
C–6I···1Br$^-$	3.318(0) (-15.6%)	166.4(1)
C–6I′···1Br$^-$	3.318(0)	162.5(0)
C–3I···2Br$^-$	3.312(0) (-15.7%)	165.0(0)
C–3I′···2Br$^-$	3.312(0)	160.0(1)
C–5I···2Br$^-$	3.489(1) (-11.2%)	163.7(1)
C–5I′···2Br$^-$	3.489(1)	160.6(0)
C–8I···2Br$^-$	3.198(1) (-18.6%)	160.0(1)
C–8I′···2Br$^-$	3.198(1)	174.4(0)
C–2I···2I–C	3.915(0) (-1.1%)	177.0(1)
C–2I′···2I–C	3.915(0)	155.3(1)
C–7I···7I–C	3.829(1) (-3.3%)	154.2(0)
C–7I′···7I–C	3.829(1)	165.7(0)
C–1H···1Br$^-$	2.963(0) (-5.9%)	139.2(0)
C–2H···1Br$^-$	2.864(0) (-9.0%)	161.2(1)
C–3H···1I–C	3.125(0) (-1.7%)	145.3(1)
C–4H···1I–C	3.178(0) (-0.06%)	141.8(1)
C–5H···3I–C	3.145(0) (-1.1%)	124.7(1)
C–6H···8I–C	3.168(0) (-0.38%)	156.4(0)
C–7H···8I–C	3.150(0) (-0.94%)	145.5(0)

The information about disordered TIE molecules

The two TIE molecules at different statistical site can well overlap crossly together in the disorder TIE/Cl$^-$ or TIE/Br$^-$ cocrystal structures, in which the lengths of C–I covalent bond are largely influenced by the kind of interactions, as shown in Fig. 4(e). In the prismatic assignment (3.573×3.573 Å) of two disordered TIEs, there are two kinds of XB (C–I···Br$^-$ and C–I···I–C) interaction, the stronger XB (the former) leads to the length of C–I covalent bond (2.173Å) longer, and the weaker XB (the latter) leads to the length of C-I covalent bond (2.069Å) shorter. In the square assignments (3.565×3.565 Å or 3.547×3.547 Å) of two disordered TIEs, only C–I···π or C–I···I–C interactions exist in a TIE, leading to the equal length of four C–I covalent bonds. In terms of the length of C–I covalent bond, the strength of C–I···Br$^-$ and C–I···π XB interactions are stronger than the C–I···I–C contact.

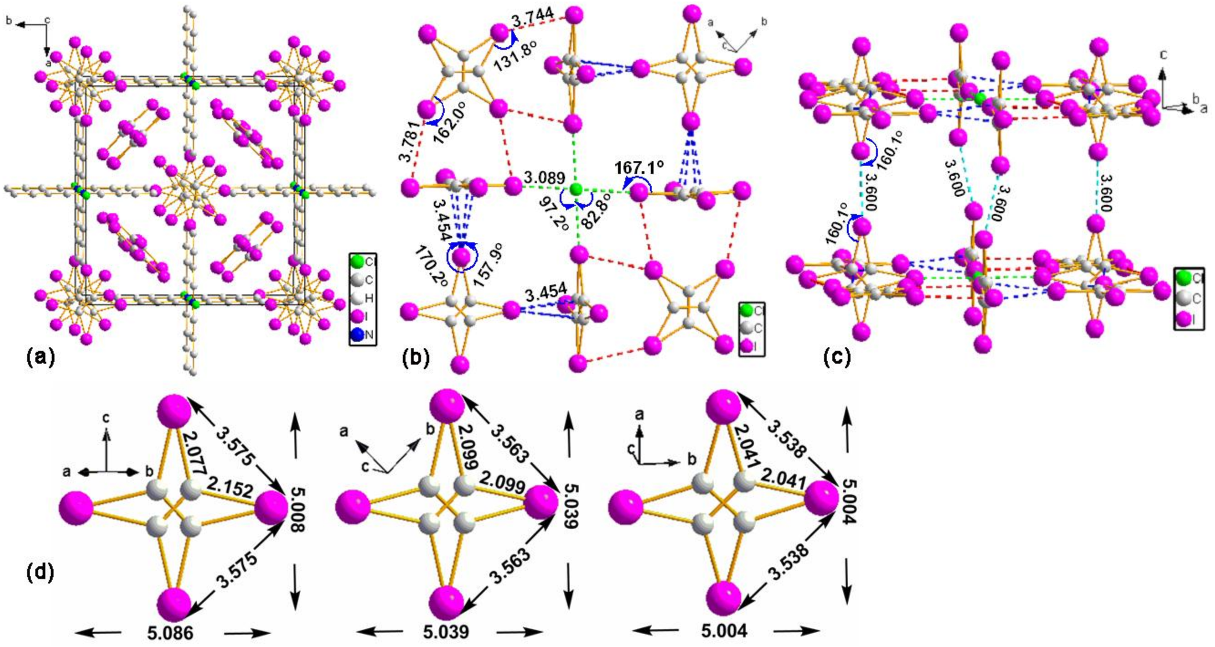

Fig. S2 Single-crystal structures of the TIE/Cl$^-$ cocrystal. (a) the crystal cell, (b) 2D-network (formed by C-I···Cl$^-$, C-I···π and type-II contacts in layer), (c) 3D-structure (connected by type-I contacts between layer-layer), (d) the arranging of two disordered TIE molecules in the TIE/Cl$^-$ cocrystal.

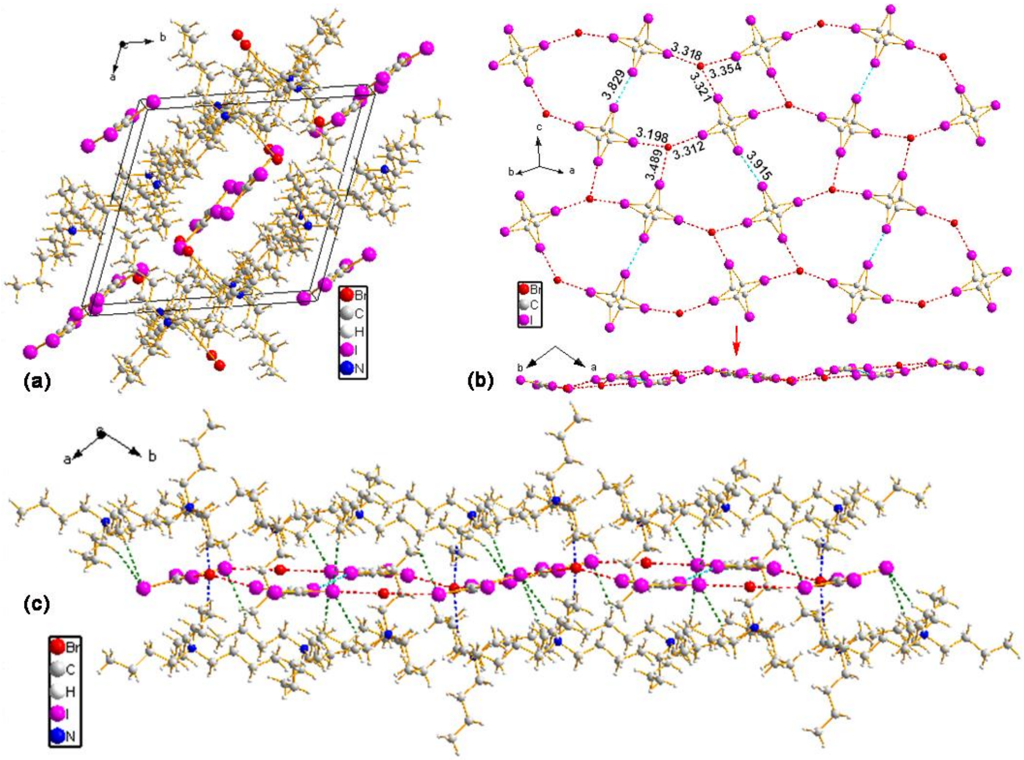

Fig. S3 Single-crystal structures of the TIE/Br$^-$ cocrystal prepared from acetone. (a) the crystal cell, (b) 2D-network (c) 3D-structure.

The structure of TIE/Br^- cocrystal obtained by slowly evaporating acetone is different from others mentioned in the article (the TIE/Br^- cocrystal from acetone has almost same cell parameters with ref,[2] but the XB lengths and angles are somewhat different). The all TIE molecules in TIE/Br^- cocrystal are disordered and the chemical composition (TIE/Br^-) and C–I/Br^- bonding stoichiometries are all 1:1. As listed in Table S3, there are six different C–I···Br^- distances with twelve different ∠C–I···Br^- bonding angles, and two different C–I···I–C distances with four different ∠C–I···I bonding angles. The 2D-network of TIE/Br^- are formed by C–I···Br^- and C–I···I–C XB interactions (*cf.* Fig. S3 (b)). When the two-dimensional direction is rotated by a certain angle (the below), it also can be seen clearly that the TIE molecules and Br^- locate in a corrugated plane. The 3D structures of TIE/Br^- cocrystal are extended by C–H···Br^- and C–H···I–C hydrogen bonding interactions (*cf.* Fig. S3 (c), the detailed discussion is described in the following section), which are not included by the previous work.[2] All these distances are well within the sum of the van der Waals radii.

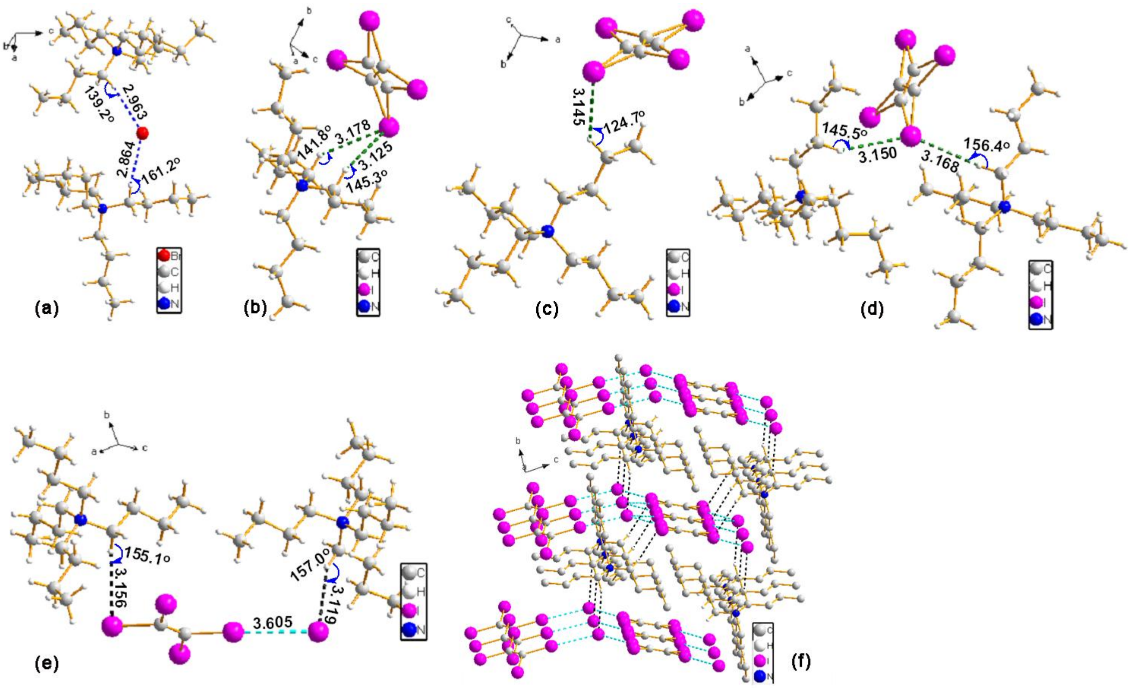

Fig. S4 Hydrogen bonding of TIE/Br$^-$ (prepared from acetone) and TIE/I$^-$ cocrystals. (a)-(d): infinite chain structures of TIE/Br$^-$ cocrystal formed by C–H···Br$^-$ and C–H···I–C interactions; (e) infinite chain structures of TIE/I$^-$ cocrystal formed by C–H···I$^-$ and C–H···I–C interactions; (f) the 3D structure of the TIE/I$^-$ cocrystal.

Fig. S4 (a) to (f) typically shows the C–H···Br$^-$, C–H···I and C–H···I$^-$ interactions. The C–H···Br$^-$ distances are 2.864 Å and 2.963 Å (9.0% and 5.9% shorter than the sum of vdW radii of H and Br$^-$) with ∠C–H···Br$^-$ bonding angles 161.2° and 139.2°, respectively. As listed in Table S3, the five different distances of three types of C–H···I–C (*cf*. Fig. S4 (b), (c) and (d), respectively) in TIE/Br$^-$ cocrystal are 3.178 Å, 3.125 Å, 3.145 Å, 3.168 Å and 3.150 Å (0.06%, 1.7%, 1.1%, 0.38% and 0.94% shorter than the sum of vdW radii of H and I) with ∠C–H···I–C bonding angles 141.8°, 145.3°, 124.7°, 156.4° and 145.5°, respectively. In TIE/I$^-$ cocrystal, the C–H···I–C and C–H···I$^-$ distance of 3.156 Å and 3.118 Å are 0.75% and 7.2% shorter than the sum of vdW radii of H and I/I$^-$, respectively. The ∠C–H···I–C and ∠C–H···I$^-$ bonding angles are 155.1° and 157.0°. The 3D structures of TIE/I$^-$ cocrystal are also extended by hydrogen bonding which are not included by the previous work.[2] All these distances are well within the sum of the van der Waals radii.

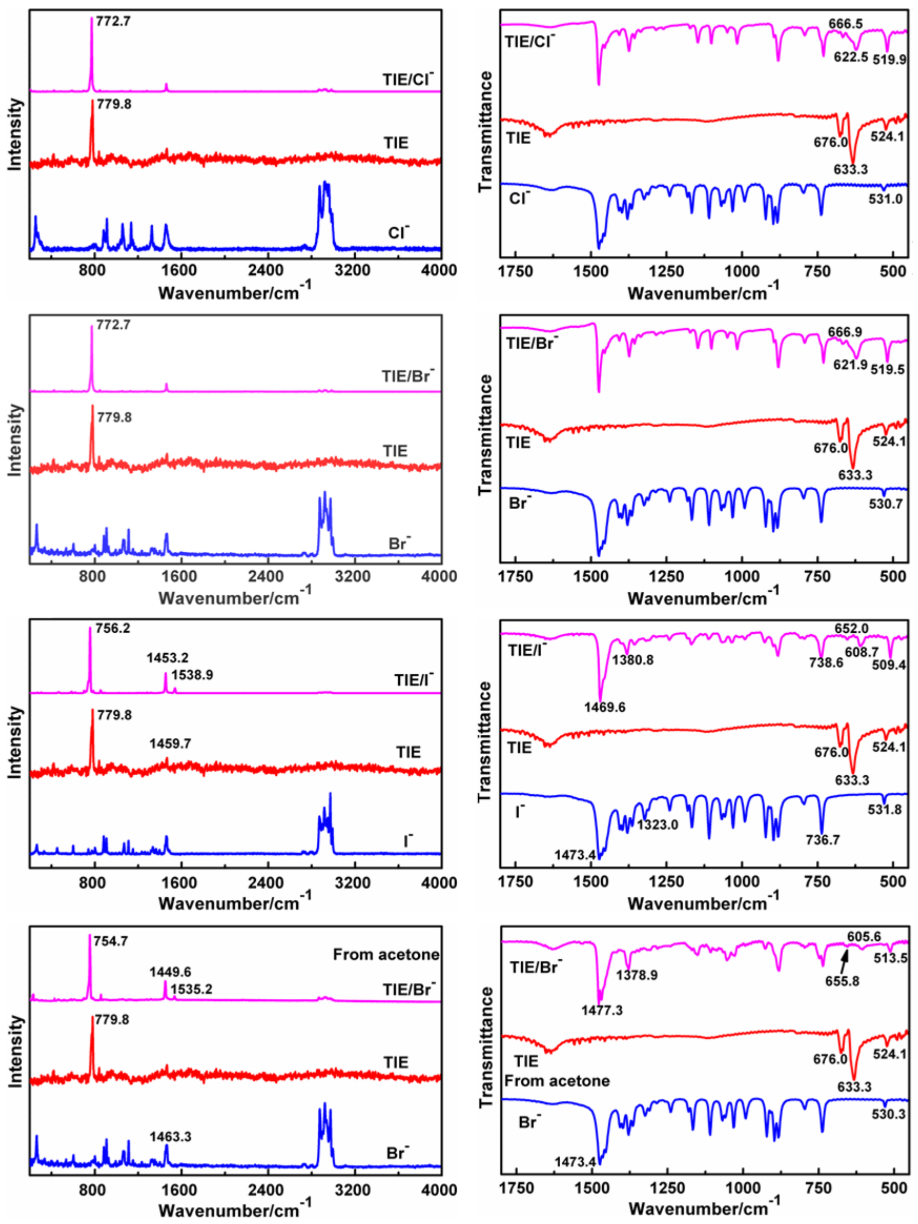

Fig. S5 Raman (left) and FT-IR (right) spectra of TIE as well as TIE/X$^-$ cocrystals.

As can be seen from the Fig. S5, the Raman band of $\nu_{C–I}$ stretching vibration is 779.8 cm^{-1} for TIE[3,4], 772.7 cm^{-1} for TIE/Cl$^-$ cocrystal, 772.7 cm^{-1} for TIE···Br$^-$ cocrystal, 756.2 cm^{-1} for TIE···I$^-$ cocrystal and 754.7 cm^{-1} for TIE/Br$^-$ cocrystal (prepared from acetone). The band in the TIE/X$^-$ cocrystal shifts to lower wavenumbers by 8 to 25 cm^{-1}. The FT-IR bands of $\nu_{C–I}$/cm^{-1} stretching vibration generally occur at 524.1, 633.3 and 676.0 for TIE,[3] while at 519.9, 622.5 and 666.5 for TIE/Cl$^-$ cocrystal, at 519.5, 621.9 and 666.9 for TIE/Br$^-$ cocrystal, at 509.4, 608.7 and 652.0 for TIE/I$^-$ cocrystal, and at 513.5, 605.6 and 655.8 for TIE/Br$^-$ cocrystal (prepared from acetone), respectively.

Changes in Raman and FT-IR bands indicate the existence of multiple hydrogen bonding: as shown in Fig. S5, the FT-IR bands of $\mathrm{Bu_4N^+{\cdot}I^-}$ are 1473.4 ~ 1454.1 cm^{-1}, 1405 cm^{-1} ~ 1363.5 cm^{-1}, 1323.0 cm^{-1}, 1240.0 cm^{-1} ~ 881.1 cm^{-1}, 794.6 cm^{-1}, 736.7 cm^{-1}, while the corresponding bands of TIE/$\mathrm{Bu_4N^+{\cdot}I^-}$ are 1469.6 cm^{-1}, 1380.8 cm^{-1}, 1355.8 cm^{-1} ~ 1168.7 cm^{-1}, 881.3 cm^{-1}, 738.6 cm^{-1}. Also the Raman active bands of $\mathrm{Bu_4N^+{\cdot}I^-}$ are 1459.7 cm^{-1}, 1395.8 cm^{-1} ~ 1261.0 cm^{-1}, 1152 cm^{-1} ~ 1069 cm^{-1}, 907.1 cm^{-1}, 881.2 cm^{-1}, and the corresponding bands of TIE/$\mathrm{Bu_4N^+{\cdot}I^-}$ are 1538.9 cm^{-1}, 1453.2 cm^{-1}, 888.4 cm^{-1} ~ 852.7 cm^{-1}. These may confirm the existence of the $\mathrm{C{-}H{\cdots}I^-}$ and C–H···I–C hydrogen bonds.

Also, for the TIE/Br$^-$ cocrystal prepared from acetone, the FT-IR bands of $\mathrm{Bu_4N^+{\cdot}Br^-}$ are 1473.4 ~ 1454.4 cm^{-1}, 1408.0 cm^{-1} ~ 1365.2 cm^{-1}, 1325.2 cm^{-1} ~ 883.1 cm^{-1}, 796.6 cm^{-1}, 738.6 cm^{-1}, 530.3 cm^{-1}, while the corresponding bands of TIE/$\mathrm{Bu_4N^+{\cdot}Br^-}$ are 1477.3 cm^{-1} ~ 1469.5 cm^{-1}, 1379.2 cm^{-1}, 1168.6 cm^{-1} ~ 927.1 cm^{-1}, 881.5 cm^{-1}, 747.8 cm^{-1}, 736.0 cm^{-1}. Also the Raman active bands of $\mathrm{Bu_4N^+{\cdot}Br^-}$ are 1463.3 cm^{-1}, 1352.6 cm^{-1} ~ 1317.6 cm^{-1}, 1152.5 cm^{-1} ~ 1061.7 cm^{-1}, 907.9 cm^{-1} ~ 603.1 cm^{-1}, and the corresponding bands of TIE/$\mathrm{Bu_4N^+{\cdot}Br^-}$ are 1535.2 cm^{-1}, 1449.6 cm^{-1}, 856.1 cm^{-1}, 754.7 cm^{-1}. These may confirm the existence of the $\mathrm{C{-}H{\cdots}Br^-}$ and C–H···I–C hydrogen bonds.

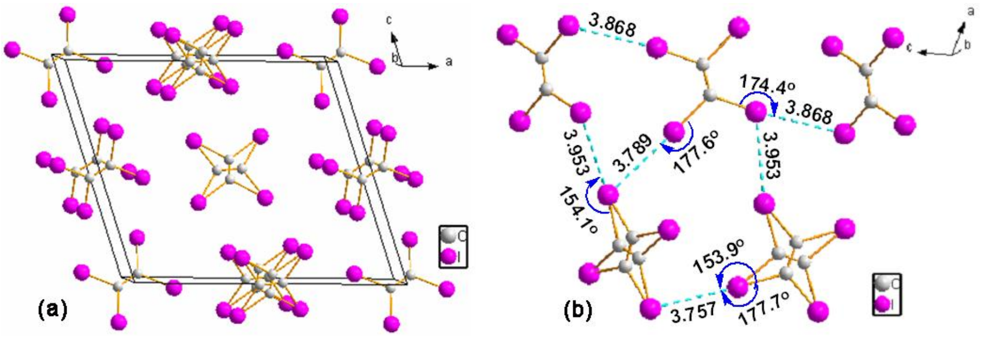

Fig. S6 The crystal cell (a) and 2-D network (b) of TIE molecules.

The calculation units of $\mathrm{C{-}I{\cdots}I^-}$ XB energies in cocrystal

The values of the energy were calculated through the unit of 2 molar $\mathrm{C{-}I{\cdots}Cl^-/Br^-}$ XB for the interaction of $\mathrm{C{-}I{\cdots}Cl^-/Br^-}$, 1 molar C-I···π XB for the interaction of C–I···π. Because of the difference of bond lengths, the values of the energy of $\mathrm{C{-}I{\cdots}I^-}$ and $\mathrm{C{-}I{\cdots}Br^-}$ (prepared from acetone) were calculated through the sum of two by two halogen bonds (*cf*. Fig. S7).

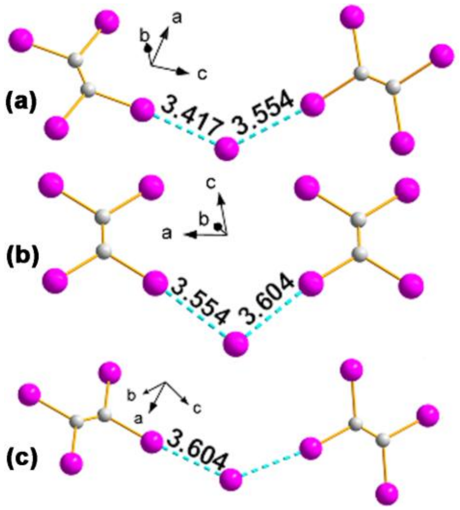

Fig. S7 The C–I···I$^-$ halogen bonding units extracted from single crystal structure data of TIE/I$^-$ for energies calculation.

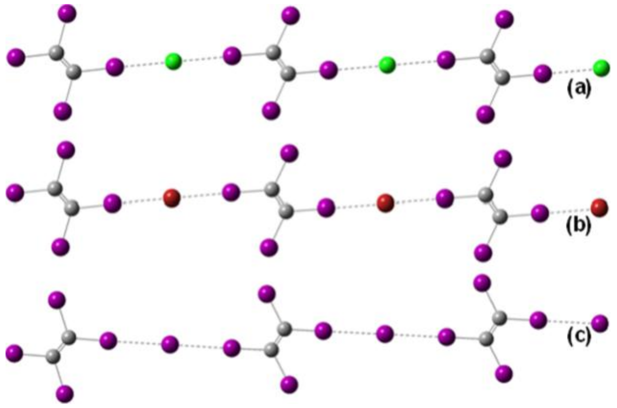

Fig. S8 Optimized structures of the XB complexes in solution. (a) TIE···Cl$^-$ complex, (b) TIE···Br$^-$ complex, (c) TIE···I$^-$ complex.

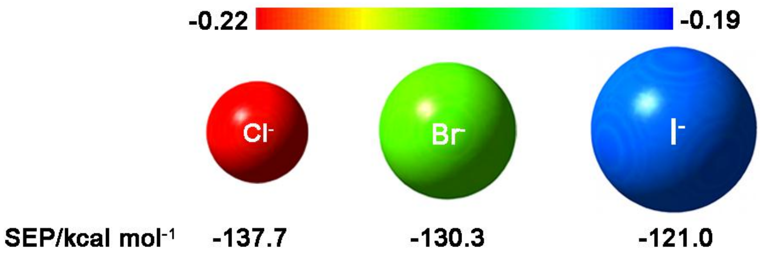

Fig. S9 The magnitudes of the negative electrostatic potential on the surface Cl$^-$, Br$^-$ and I$^-$.

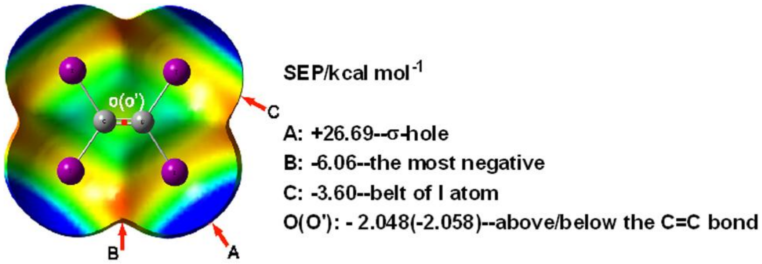

Fig. S10 The calculated electrostatic potential surface of TIE molecule. Blue: positive region; Green: electroneutral region; Red: negative region.

The reason of alert level A in the checkCIF report of TIE/I$^-$

This issue may occur due to the existence of C–I···I-C halogen bonding, which cause that the C–I···I-C distance is shorter that twice vdW radii of I.

References

[1] Q. M. Mou, Y. Peng, Z. G. Zhao and S. H. Chen, *Chin. J. Org. chem*. 2004, **9**, 1018-1028.

[2] H. Bock and S. Holl, *Z. Naturforsch.* 2002, **57b**, 713-725.

[3] R. Forneris and M. Uehara, *J. Mol. Struct.*, 1970, **5**, 441-447.

[4] The Raman shift at 779.8 cm^{-1}, in fact, is a multiple peak, reflecting the inequality of the C–I covalent bonds and the different interactions in TIE crystal or cocrystals. (*cf*. Fig. S6: TIE crystal).